

Numerical Modelling of Sediment Transport Caused by Deep Sea Mining

W. ZIELKE, J.A. JANKOWSKI
University of Hannover, Germany

J. SÜNDERMANN, J. SEGSCHEIDER
University of Hamburg, Germany

Abstract

The paper describes the application of mesoscale and large scale models in order to simulate the impact of deep sea mining sediment discharges on the marine environment. The modelling efforts are crosslinked with the experiments of the TUSCH research group which provide supporting data. The results yield time-dependent and three-dimensional concentration fields, the amount of redeposition, and the plume residence time. The emissions at the bottom lead to an impact mainly at a local scale, whereas contamination in the larger areas due to discharges at the free surface or in some intermediate depth cannot be excluded.

Keywords

Deep sea mining, environmental impact assessment, sediment transport, hydrodynamic numerical modelling, large scale geostrophic model, Pacific Ocean

Introduction

The results of the mesoscale and large scale modelling described in this contribution were achieved within the research activities of the interdisciplinary research group TUSCH (from German: Tiefseeeumweltschutz, deep sea environment protection). For its background, scientific aims, research program and achievements, as well as environmental aspects of the deep sea mining the reader is referred to Thiel et al. and Schriever, this issue. From all the possible dangers for the deep sea environment, the activities of the TUSCH group concentrate on the assessment of impacts caused by the exploitation of manganese nodule deposits.

Assessing the environmental impact of human activities in the deep sea was the topic of numerous research works in the past, with special attention to the nuclear waste dumping. In contrast to dumping, commercial exploitation of the manganese nodule deposits is still a matter of unforeseeable future (Thiel et al., this issue). The deposits were intensively explored and researched in the past twenty years and the appropriate mining technologies have been developed and tested in many countries, showing that deep sea mining is feasible from the technological point of view (e.g. Bischoff and Piper, Eds., 1979; Halbach et al., Eds., 1988; Kunzendorf, 1988).

Field mining tests have shown in the past, however, that even with the most modern technologies, mining of the manganese nodules will inevitably be accompanied by destruction of the sea floor and by a resuspension of some bottom sediments as well as ore particles (Lavelle et al., 1981; Lavelle et al., 1982; Thiel, 1991). Depending on the mining technology, the discharges will take place in different depths and with different intensity, mainly during nodule harvesting directly at the bottom or as mining tailings (wastes). The generated sediment plumes will be further transported with the ocean currents and, at worst, form stable turbidity layers in different depths (Ozturgut et al., 1981; Baturin et al., 1991). A chronic exposition of marine organisms to great amounts of particles in concentrations exceeding ambient oceanic concentrations or being of unusual origin is expected to occur (particulate pollution). Therefore, one problem of the environmental impact assessment is to estimate how long the plume persists before it eventually dilutes to approximately the ambient concentration level or settles at the bottom.

The aim of the research described in this contribution is to develop numerical sediment transport models in connection with the potential deep-sea mining activities in a reference area located in the South-Eastern equatorial Pacific Ocean off Peru. In this region, a German mining claim is registered and field works of the TUSCH research group are carried out in order to obtain the required scientific background for evaluating the deep sea mining impacts and to provide the necessary supporting data for the modelling (Thiel and Schriever, 1989; Thiel, 1991).

The modelling effort is directed on one hand to provide a tool which will allow reliable risk assessment in the near field and in the mesoscale, where the greatest impact is expected and, on the other hand, in the large scale, where the long-term effects are being studied. This complementary approach of two research groups from universities of Hamburg (large scale) and Hannover (mesoscale), being an integral part of TUSCH project and crosslinked with its other activities, allows simulations in the time scales of hours to weeks as well as from months to years.

The Near Field and Mesoscale Model

The aim of the mesoscale group is to develop a model which will provide reliable risk assessment of the discharges in the near field and in the mesoscale, i.e. in the time scales from hours to weeks. According to this, a mesoscale regional model was developed for a reference area situated in the Peru Basin in the Southeast Pacific Ocean (ca. 450 km², centered about 7° 04'S, 88° 28'W). In this region the experimental activities of the TUSCH group, providing the supporting data, are carried out (DISCOL Experimental Area, DEA, Thiel and Schriever, 1989). The size of this region allows a simulation of a plume spreading during 1–2 weeks, depending on the current strength. The computational mesh consists of almost 10⁵ prismatic 3D-elements, providing horizontal resolution of 500–700 m, except in the direct vicinity of the emission (100 m). In the vertical direction the mesh planes are logarithmically distributed near the bottom and uniformly up to 500 m above it, so that the bottom boundary layer is appropriately resolved (1–100 m). The technology assumed in the simulation is that of remote-controlled, self-driving nodule collectors on the ocean floor, which collect and prepare the nodules for transport to the surface through a riser system (Kunzendorf, 1988). This technology limits the discharges mainly to the bottom boundary layer of the ocean.

The mesoscale model takes into account all relevant physical phenomena in the deepest zone of the ocean and yields results which describe the time-dependent, three-dimensional concentration fields, including the amount of redeposition and the plume residence time (Jankowski et al., 1995). The main accent is put on the simulation of the mesoscale hydrodynamic phenomena. Indeed, the analysis of the long-term current measurements in the DISCOL Area (Klein, 1993) reveals that the main hydrodynamic features to be described for simulation of this area are the currents in a geostrophic equilibrium, long gravity waves in the inertial and tidal frequency range that may be treated as a perturbation of the geostrophic balance state and the bottom boundary layer. So-called benthic storms were not observed; current speeds of over 10 cm/s were detected only during a few hours. Fig. 1 gives an illustration of the current variability during the first year of measurements.

Due to the spatial limits of the model, concentration on the features of the deepest zone of the ocean as well as the fact that the boundaries of the computational area are open, the forces generating the current variability are not simulated directly. The current variability is obtained by applying and calibrating varying pressure fields on the limits of the area, and applying appropriate initial conditions for velocity and surface elevation (LeBlond and Mysak, 1978). An example for a comparison between the modelled and measured velocity components on the level 50 mab for the days 330–340 with a relatively strong current (compare fig. 1) is given in fig. 2.

The hydrodynamic and transport model is based on the incompressible Navier-Stokes equations with the free surface boundary condition and the transport equation for sediment. The algorithm of the finite-element code, TELEMAC-3D (LeNormant et al., 1993), is based on the operator-splitting method. The equations are split into fractional steps with respect to the physical processes and treated by appropriate numerical methods. The code is fully vectorised and takes advantage of the capabilities of modern supercomputers.

The momentum and continuity equations to be solved are obtained using the Boussinesq approximation and neglecting inertial effects in the vertical direction. The roughness of the bottom is taken into account through the Chézy formulation. The vertical eddy viscosities and diffusivities are described by a mixing-length model with damping functions, while horizontal values are constant. The parameter controlling vertical distribution of the mixing length is applied to determine the vertical distribution of the eddy viscosity as well as bottom boundary layer thickness.

The stratification phenomena are taken into account by using damping functions derived from a second-order turbulence model. The CTD profiles in the deepest zone of the DISCOL area show an almost constant temperature and salinity (Thiel and Schriever, 1989). Stratification is very weak but stable. Therefore, an assumption of neutral stratification is taken for modelling the velocity profile in

Class	d_i μm	$\Delta\rho$ kg/m^3	w_{s_i} m/s	$n(d_i)$	$nm(d_i)$
a	100	76.7	$2.41 \cdot 10^{-4}$	0.14	0.7933
b	80	102.5	$2.06 \cdot 10^{-4}$	0.03	0.0890
c	50	192.2	$1.51 \cdot 10^{-4}$	0.07	0.0547
d	30	238.2	$6.74 \cdot 10^{-5}$	0.36	0.0630
e	3	626.5	$1.77 \cdot 10^{-6}$	0.40	0.0001

Table 1: DISCOL sediment classes with their settling velocities.

the BBL over smoothly varying bottom without presence of the suspended matter. In the following, only the suspended sediment is assumed to be able to affect the water density, causing stronger stratification or density currents.

The sediment transport equation is being solved by the operator-splitting method, as well. The probabilities for deposition and erosion are defined according to (Krone, 1962) using empirical parameters. In this study it is assumed that no erosion of the deep-sea bed occurs in the low energetic bottom boundary layer, and the probability of deposition is one, i.e. each sediment particle reaching the bottom will be deposited (Jankowski et al., 1995).

The model can be calibrated to specific experimental data, especially in the case of the bottom boundary hydrodynamics and settling velocity formulation. The model is developed independently of the particular location and is applicable also to other areas of potential deep sea mining. Verification and input data from the mining tests or other specific experiments are scarce, and there are still uncertainties in the model parameters (Lavelle et al., 1981; Trueblood, 1993; Brockett and Richards, 1994).

In order to simulate the transport in the DISCOL area caused by a discharge from a single collector, the parameters with only approximately known values are varied within an acceptable range. Several current scenarios representative for this region, different mean settling velocities, or a composite spectrum of settling velocities and different parameters controlling the thickness of the bottom boundary layer, velocity profile and vertical diffusivity are taken into account. Various aspects affecting the plume transport and sedimentation, such as gravity currents and flocculation in a sediment-laden water column, and the hydrodynamics of the area are discussed.

The parameter studies show that the behaviour of the suspended sediment under the conditions of the oceanic bottom boundary layer (BBL) depends mainly on the vertical diffusivity and on the settling velocity of the sediment particles. An additional settling effect is caused by the density currents, which generate near-bottom, flat distribution of the plume in the initial stages after discharge. The stratification caused by the suspended sediment dampens the vertical mixing (Jankowski et al., 1994).

One of the most important parameters controlling the plume spreading is the mean settling velocity of the discharged sediment particles. The published particle size distribution from the first centimetre of the DEA (Klein, 1993) can be assumed as adequate for the distribution in the discharged plume. The values for the Stokes' settling velocities of sediment classes from DEA-region are given in table 1. They are computed according to the method described in (McCave, 1984) where $w_s = \Delta\rho g d^2 / 18\mu$, ($\Delta\rho$ is the density contrast, i.e. difference between particle in-situ density minus surrounding fluid density, $\mu = 1.7 \cdot 10^{-3}$ kg/ms the in-situ dynamic viscosity of sea water). The density contrast given by (McCave, 1984) can be also applied to compute the mass percentage distribution $nm(d)$ from the given percentage diameter distribution $n(d)$ from DEA. From the given mass distribution, the mean settling velocity of the composite sediment spectrum can be estimated using

$$w_{sm} = \frac{\sum_i w_{s_i} c_i}{\sum_i c_i} \quad (1)$$

where c_i are the dry mass concentrations of the constituent, characterized by diameter d_i . Taking the diameter values in the middle of intervals defined in table 1 as d_i , the value of 3 μm for the finest particles and the limit value of 100 μm for the largest, the lowest value for the mean velocity of this sediment distribution will turn out to be $w_{sm} \approx 2.2 \cdot 10^{-4}$ m/s.

Because of the importance of the settling velocity in the transport of the suspended sediment, special attention was paid to the flocculation and breakup processes of cohesive sediment particles (McCave,

1984). The data depicting the particle size distribution from the DEA (Klein, 1993) show that the percentage frequency distribution of the particle diameters $d < 60\mu\text{m}$ equals ca. 83% (table 1). The possibility of applying an empirical model for the mean settling velocity (Malcherek et al., 1994) was tested. Due to the conditions in the low energetic ocean bottom boundary layer (Monin and Ozmidov, 1985), the flocculation phenomena depend mainly on the differential settling of the different size sediment particles and Brownian motion and turbulent shear influences can be neglected (Jankowski et al., 1995). Therefore, as soon as the supporting data are available, an empirical model will be applied and verified, in which the settling velocity is a function of the sediment concentration. The possible flocculation effects may, therefore, only accelerate the deposition compared to the non-cohesive case, since the break-up effects are insignificant. Nevertheless, it should be mentioned that higher concentrations, with stronger flocculation effects, are found in the vicinity of the collector only. Consequently, flocculation may be unimportant in the diluted plumes at a greater distance from the source. Therefore in the simulations different constant mean settling velocities (with the most realistic value 10^{-4}m/s) or a composite spectrum of settling velocities for non-cohesive sediment classes ($a - e$) according to table 1 are assumed for conservative residence time estimations in the mesoscale.

For constant settling velocities in the range of 10^{-4}m/s the emissions at the ocean bottom lead to an impact mainly at a local scale. The residence time can be defined as the time in which the resuspended mass is diminished by a factor of $1/e$, i.e. when 63% of the suspended mass has deposited. The results for a sediment plume discharged by a single collector for 24 hours at a rate of 10 kg/s and moving along a straight linear path in alternate directions in a relatively small area of ca. 4 km^2 show that the residence time is within the range of 1–6 days. Similar values are obtained when using a composite spectrum of settling velocities or for a continuous discharge. The ambient sediment concentration is assumed to be 0.01 mg/l in the Peru Basin. Depending on the parameter values, the maximum sediment concentration in the plume after 6 days, will differ between the values 1–50 times greater than the ambient concentration for the time-limited case. The studies with the composite spectrum of sediment classes show that this diluted plume consists of the finest particles with low settling velocities (fig. 4). By continuous 6 days' discharge, a plume is formed where the concentration falls to the ambient value about 15 km from the source. In all cases the bottom is covered with high amounts of sediment (deposition greater than 100 g/m^2 , i.e. about 0.5 mm thickness) in the radius of 1–2 km off the collector tracks (Jankowski et al., 1995).

As an example, the horizontal sections (at approximately 1 m above bottom, fig. 3) of sediment plumes (24 h emission) in development for the time moment of 3 days (72h) are shown, as well as the redeposition pattern in the neighbourhood of the test area. The constant mean settling velocities are $1 \cdot 10^{-4}\text{ m/s}$ and $5 \cdot 10^{-5}\text{ m/s}$, showing an effect of taking different mean settling velocities in the deposition pattern and concentration distribution.

The Large Scale Model

In the large scale working group, the sediment transport is modelled with a Lagrangian or particle tracing model. The theoretical approach, as given e.g. by Einstein (1905), is the solution of a Fokker-Planck equation:

$$\frac{\partial p}{\partial t} + \frac{\partial}{\partial x_i}(\bar{u}_i p) - \frac{\partial}{\partial x_i} \left(\frac{\sigma}{2t} \frac{\partial p}{\partial x_i} \right) = 0 \quad (i = 1, 3) \quad (2)$$

with p the probability to find a particle at (\vec{x}, t) , x_i are the components of the vector describing the position of the particles, \bar{u}_i the components of the mean velocity over the ensemble of particles and σ the standard deviation of the ensemble of particles with respect to location. σ^2 is given by $\frac{1}{N} \sum_{n=1}^N (\vec{x}_n - \bar{\vec{x}})^2$, where \vec{x}_n are the locations of the individual particles, and $\bar{\vec{x}}$ is the mean position of the particle cloud, and N the total number of particles. The exchange coefficient A_i is then determined by $\sigma_i/2t$.

Thus, the second term in (2) represents advection and the third term mixing by subgridscale turbulence. In the practical approach, the advective velocities are taken from a global ocean circulation model developed at the Max-Planck-Institut für Meteorologie in Hamburg (Maier-Reimer et al., 1993). General features are the $3.5^\circ \times 3.5^\circ$ horizontal resolution and the time step of one month. For the present work, the output of a 22-layer version of the model (Mikolajewicz, pers. comm) is used in contrast to the eleven-layer version described in Maier-Reimer et al. (1993). The thickness of the deepest layer is adjusted to the real topography and the mean thickness is 500 m in the investigated area. The model is

forced by observed winds (Hellermann and Rosenstein, 1983) and air temperature from the COADS data set (Woodruff et al., 1987) as well as freshwater fluxes that were gained in a spin-up run relaxed to annual mean salinity (Levitus, 1982). Fig. 5 gives an example for the current field in 3500 m depth. At the DEA site, we find that the current is directed towards the northwest with velocity of less than one cm/s. To the west of the DEA-site, easterly currents prevail with velocities of 2–3 cm/s.

The turbulent mixing term in (1) is realized by the use of a random number generator with a given bandwidth. The random numbers are centered around zero. The bandwidth determines the size of the exchange coefficient. This is actually achieved by scaling the random numbers by a given factor. Fig. 6 shows the resulting probability density P , depending on distance Δx from the source and time t . The initial condition is $P(t = 0, x = 0) = 1$. In Fig. 6a, only the dispersion of the particles can be seen, while in Fig. 6b the additional advective velocity shifts the mean position of the cloud. The approach has been used successfully e.g. in the North Sea (Sündermann, 1993; Sündermann, 1994) and has special advantages in the case of strong concentration gradients of passive tracers and also for point sources compared to Eulerian calculations. The main disadvantage is the large number of particles required to satisfy the laws of statistics, thus needing a large amount of computer memory. The actual source code runs on the C90 at the DKRZ in Hamburg and requires the memory of 16 Mw. The time used to integrate 50 model years is roughly 15 minutes.

An example for the development of the particle cloud in time is shown in Fig. 7. Here a constant settling velocity of 10^{-7} m/s has been used. The source is located at 8.75° S, 82° W and at 2500 m depth. The heavy dots show the mean position of the cloud at time t (in yearly intervals), the lines show the horizontal standard deviation every five years. The total time shown is 500 years. At the end of the integration time we find that the mean position changes only slowly as in the deeper layers the advective currents slow down. Also the zonal extent of the cloud prevails over the meridional one, as can be seen from the respective components of the standard deviation.

In the application for deep sea mining, the particles do have a settling velocity according to their diameter. The frequency distribution of the diameters is given by data from Schriever (published in Klein, 1993) and represents the uppermost centimeter of sediment in the DEA (DISCOL Experimental Area). Two model runs were performed with the particle diameter frequency distribution. A continuous source was assumed with 100 particles per timestep, released at 90° W, 10° S. In Fig. 8 two zonal sections along 5° S show the resulting concentrations for (a) surface and (b) near bottom release. The figure represents the integral over 100 years, that means all areas affected within 100 years are shown. The plume to the east in Fig. 8a shows the rapid sinking of the largest particles and has a lifetime of about 2 years. The discontinuous contours arise from the distribution of the particles in settling velocities classes. Further to the West, the next class of particles is resettling about 3000 km away from the source while the finest particles are drifting as far as 10000 km into the Western Pacific. For the deep sea release (Fig. 8b), the spreading of the particles is far more restricted to the vicinity of the source. Within about 1000 km the main part resettles, and only very low concentrations are found at a greater distance. The results should be treated in a qualitative way, as the amount of resuspended sediment is still unknown. Further improvements of the initial conditions are hoped to be gained during the planned experiment EXPERU.

Summary and Future Developments

The results of the mesoscale model show that emissions at the bottom lead to an impact mainly at a local scale, while by the discharges at the free surface or in some intermediate depth, simulated with the large scale model, a contamination in the larger areas cannot be excluded. The results of the mesoscale model are valid for comparatively limited emissions, such as during mining tests or impact experiments. Under these assumptions, the results show that in the future studies of the environmental impact, direct and unavoidable destruction of the sea floor, changes in the chemical milieu or heavy metal release may be equally important as the influence of the bottom sediment plumes. Nevertheless, a tailings discharge near the ocean surface or at some intermediate depth lead to different conclusions. From the large scale investigation, it was found that fine-grained particles spread over distances of more than 1000 km if released 500 m above bottom, and even further when discharged near the surface. The main part of the sediment resettles at a distance up to about 250 km from the source. The surface discharge (if any) should be made at least below 700 m to avoid a drift of the particles towards the South American coast with the Equatorial Undercurrent.

Further development of the both models will also include the simulation of the transport of other

discharged substances interacting with the suspended sediments, for example heavy metals released from the nodules. Experiments to obtain the interaction parameter values, as well as supporting data for the settling velocity modelling and current measurements in the BBL, are to be performed during the planned TUSCH-experiments (EXPERU). The large scale modelling will use in the future also transient boundary conditions for wind and air-temperature to learn about the natural variability of oceanic conditions in the Eastern equatorial Pacific and thus about the transport paths.

The overall aim of the modelling part of the TUSCH research is to provide tools which will allow extrapolation and evaluation of the experimental results of a joint, interdisciplinary research group in order to formulate an environmental impact statement depicting the deep-sea mining operations.

Acknowledgements

The research work described in this article was sponsored by the German Federal Ministry for Science and Technology (BMFT) within the interdisciplinary research group TUSCH and under Grants No. 03F0010A and No. 03F0010B. The authors are responsible for the contents of this paper. The mentioned code TELEMAC3D was developed by Electricité de France.

References

- Baturin, G., Demidova, T., Kontar', Y., and Kurlayev, N., 1991. The recovery and processing of the iron-manganese nodules and the turbidity of the bottom layer of the ocean. *Oceanology*, **31**(4), 473–481.
- Bischoff, J., and Piper, D., Eds., 1979. *Marine Geology and Oceanography of the Pacific Manganese Nodule Province*, Plenum Press. 839 pp.
- Brockett, T., and Richards, C., 1994. Deepsea mining simulator for environmental impact studies. *Sea Technology*, **1994**(8), 77–82.
- Einstein, A., 1905. Über die von der molekularkinetischen Theorie der Wärme geforderte Bewegung von in ruhenden Flüssigkeiten suspendierten Teilchen. *Annalen der Physik*, **IV**.
- Halbach, P., Friedrich, G., and Stackelberg, U., v., Eds., 1988. *The manganese nodule belt of the Pacific Ocean*, Enke Verlag, Stuttgart. 254 pp.
- Hellermann, S., and Rosenstein, M., 1983. Normal monthly wind stress over the World Ocean with error estimates. *Journal of Physical Oceanography*, **13**(7–12), 1093–1104.
- Jankowski, J., Malcherek, A., and Zielke, W., 1994. Numerical modelling of sediment transport processes caused by deep sea mining discharges. In *Proceedings of the OCEANS 94 Conference, Brest*, vol. III, IEEE/SEE, pp. 269–276.
- Jankowski, J., Malcherek, A., and Zielke, W., 1995. Numerical modelling of suspended sediment due to deep sea mining. Submitted to *Journal of Geophysical Research – Oceans*.
- Klein, H., 1993. Near-bottom currents in the deep Peru Basin, DISCOL Experimental Area. *Deutsche Hydrographische Zeitschrift*, **45**, 31–42.
- Krone, R., 1962. Flume studies of the transport of sediment in estuarial shoaling processes. Final report, Hydraulic Engineering Laboratory, University of California, Berkeley.
- Kunzendorf, H., 1988. Proposed marine mineral exploration strategies for the nineties. *Marine Mining*, **7**, 233–247.
- Lavelle, J., Ozturgut, E., Baker, E., and Swift, S., 1982. Discharge and surface plume measurements during manganese nodule mining tests in the North Equatorial Pacific. *Marine Environmental Research*, **7**, 51–70.
- Lavelle, J., Ozturgut, E., Swift, S., and Ericson, B., 1981. Dispersal and resedimentation of the benthic plume from deep-sea mining operations: a model with calibration. *Marine Mining*, **3**(1/2), 59.
- LeBlond, P., and Mysak, L., 1978. *Waves in the ocean*. Elsevier Oceanography Series 20. Elsevier, Amsterdam–Oxford–New York. 602 pp.

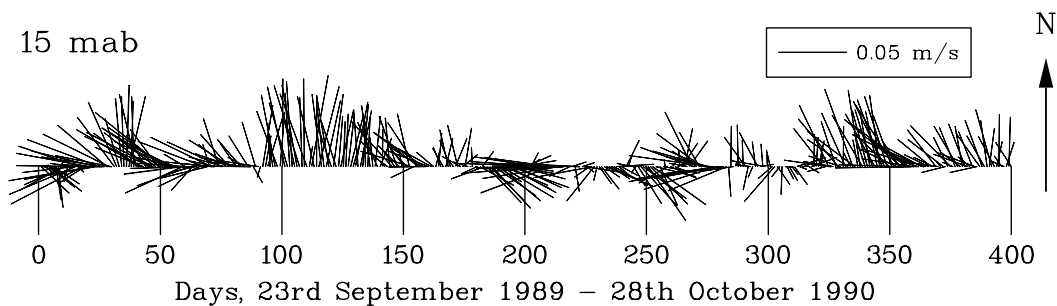


Figure 1: Stickplot of daily averages of measured velocity vectors in the Discol Area (15 m above bottom), after (Klein, 1993).

- LeNormant, C., Lepeintre, F., Teisson, C., Malcherek, A., Markofsky, M., and Zielke, W., 1993. Three dimensional modelling of estuarine processes. In *MAST Days and Euromar Market, Project Reports Volume 1*, K.-G. Barthel, M. Bohle-Carbonell, C. Fragakis, and M. Weydert, Eds., Brussels.
- Levitus, S., 1982. Climatological Atlas of the World Ocean. *Prof. Pap.*, 13, National Oceanic and Atmospheric Administration, Rockville, Md.
- Maier-Reimer, E., U., M., and Hasselmann, K., 1993. Mean circulation of the Hamburg LSG OGCM and its sensitivity to the thermohaline surface forcing. *Journal of Physical Oceanography*, 23(4), 731-757.
- Malcherek, A., Markofsky, M., and Zielke, W., 1994. Numerical modelling of settling velocity variations in estuaries. *Archiv für Hydrobiologie, Beihefte Ergebnisse der Limnologie*. in press.
- McCave, I., 1984. Size-spectra and aggregation of suspended particles in the deep ocean. *Deep-Sea Research*, 31.
- Monin, A., and Ozmidov, R., 1985. Turbulence in the ocean. D. Reidel Publishing Co., Dordrecht, Boston, Lancaster. 247 p.
- Ozturgut, E., Lavelle, J., and Erickson, B., 1981. Estimated discharge characteristics of a commercial nodule mining operation. *Marine Mining*, 3(1/2), 1-13.
- Sündermann, J., 1993. Suspended particulate matter in the north sea: Field observations and modell simulations. *Phil. Trans. R. soc. Lond. A.*, 343, 423-430.
- Sündermann, J., Ed., 1994. Circulation and contaminant fluxes in the North Sea, Springer Verlag, Heidelberg. 654 pp.
- Thiel, H., 1991. From MESEDA to DISCOL: a new approach to deep-sea mining risk assessments. *Marine Mining*, 10, 369-386.
- Thiel, H., and Schriever, G., 1989. Cruise report DISCOL 1, SONNE-cruise 61. Report Nr. 3, Zentrum für Meeres- und Klimaforschung der Universität Hamburg. 75 pp.
- Trueblood, D., 1993. US Cruise report for BIE II. NOAA Technical Memorandum NOS OCRM 4, NOAA, National Ocean Service.
- Woodruff S.D., Slutz, R.J., Jenne, R.L., and Steurer, P., 1987. A comprehensive ocean atmosphere data set. *Bull. Am. Meteorol. Soc.*, 68, 1239-1250.

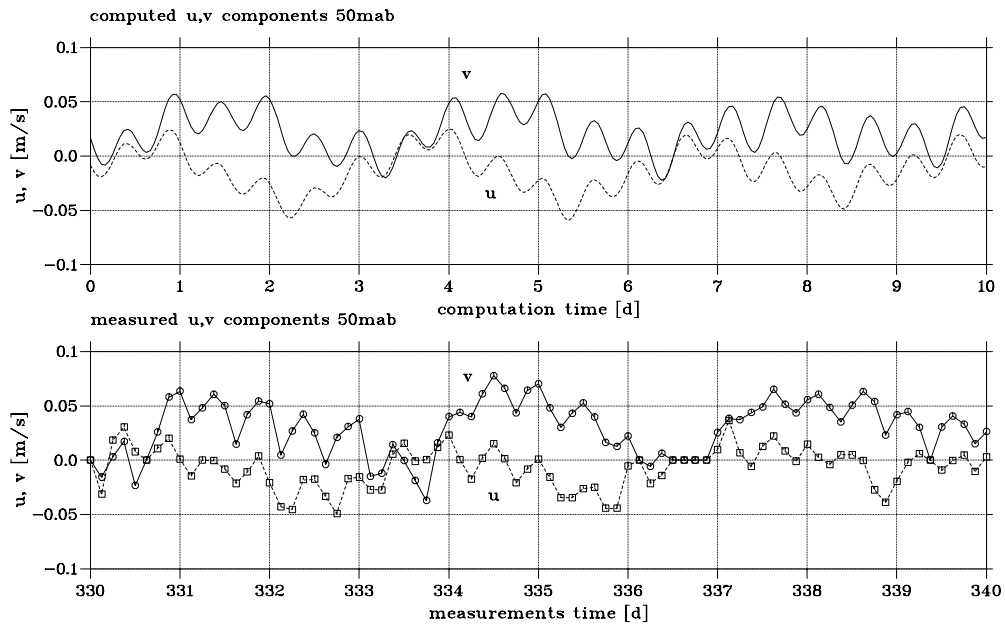


Figure 2: A comparison between the velocity components in the model and in the measurements at the level 50 mab for the days 330–340.

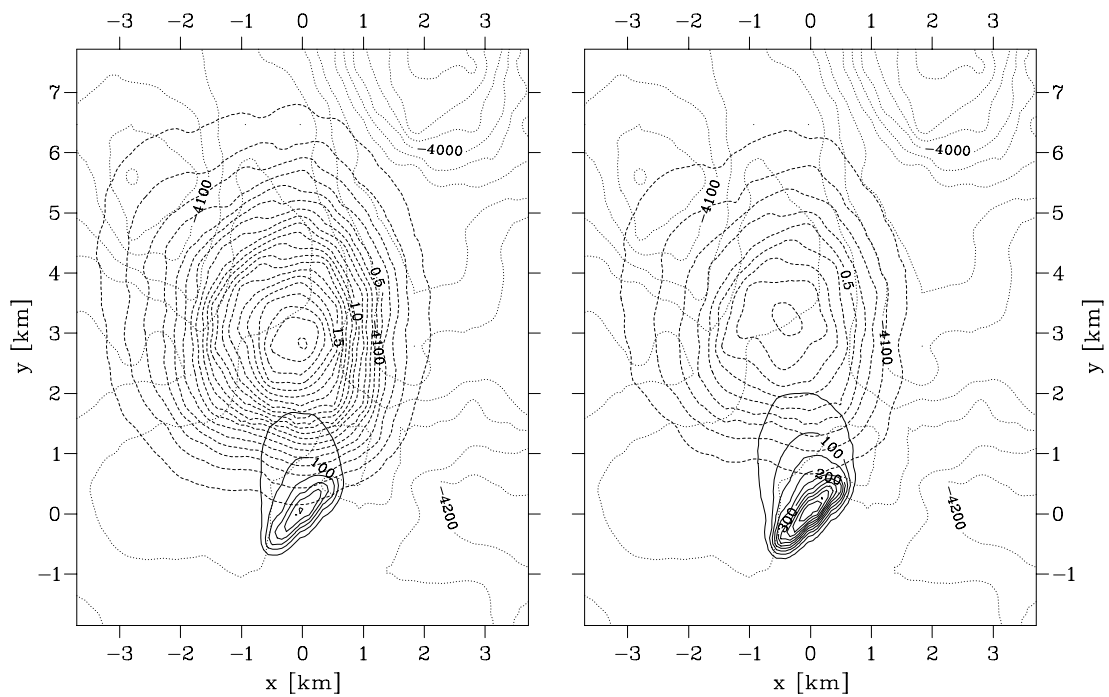


Figure 3: A horizontal cut 1 m above bottom of sediment plumes and the resedimentation patterns for the time moment 72h. The units for the concentration are mg/l and for the deposition g/m^2 .

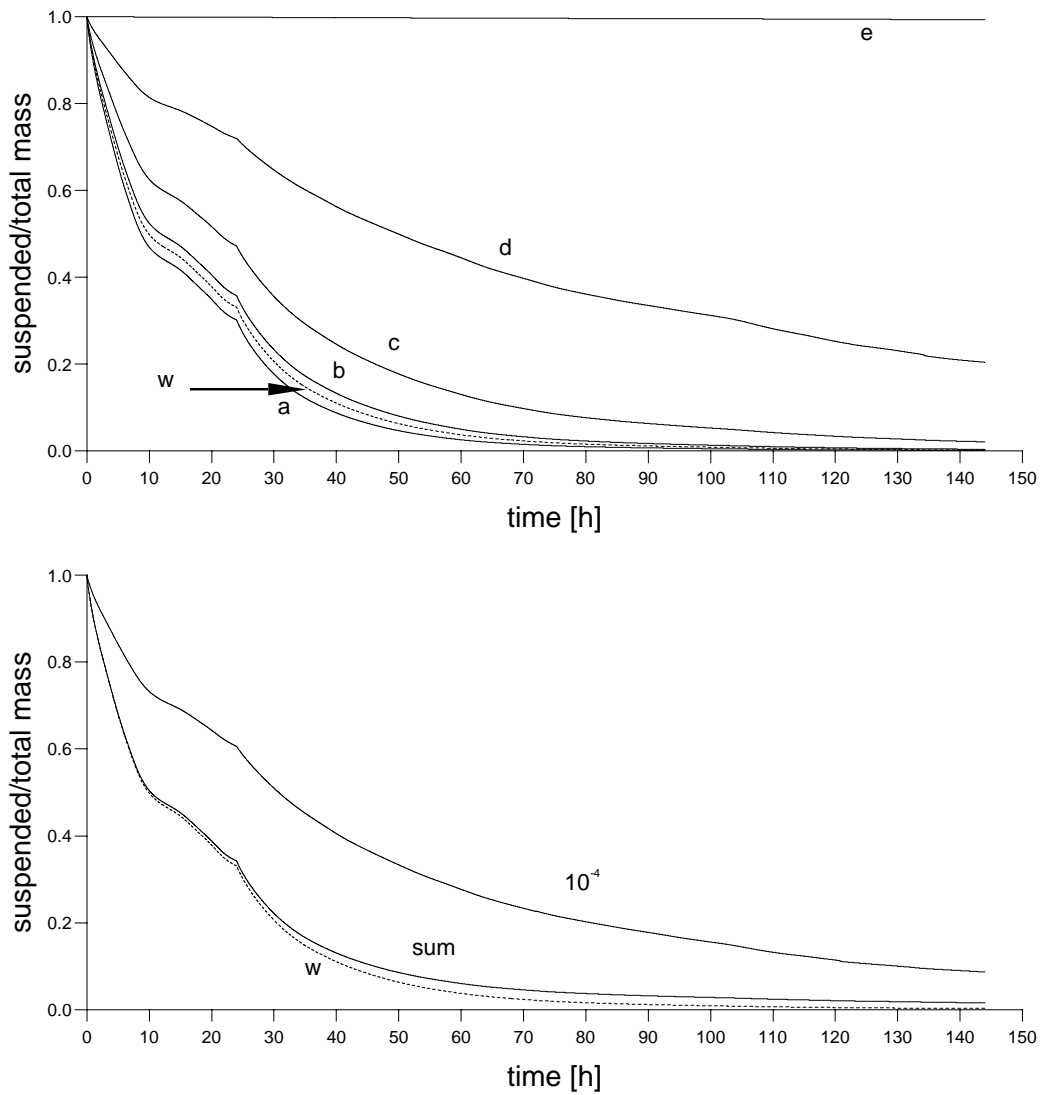


Figure 4: The removal of the sediment from the water column for time-limited emission (24 h). The results for sediment fractions a, b, c, d, e are being compared with the results for the mean settling velocity of DEA sediment ($w, 2.2 \cdot 10^{-4}$ m/s) and for the composite spectrum of settling velocities sum . The curve 10^{-4} illustrates settling with $w_s = const = 1.0 \cdot 10^{-4}$ m/s.

Figure 5: Current vectors from layer 18 of the 22-Layer LSG, i.e. in 3500 m depth. The velocity scale is in the upper right corner.

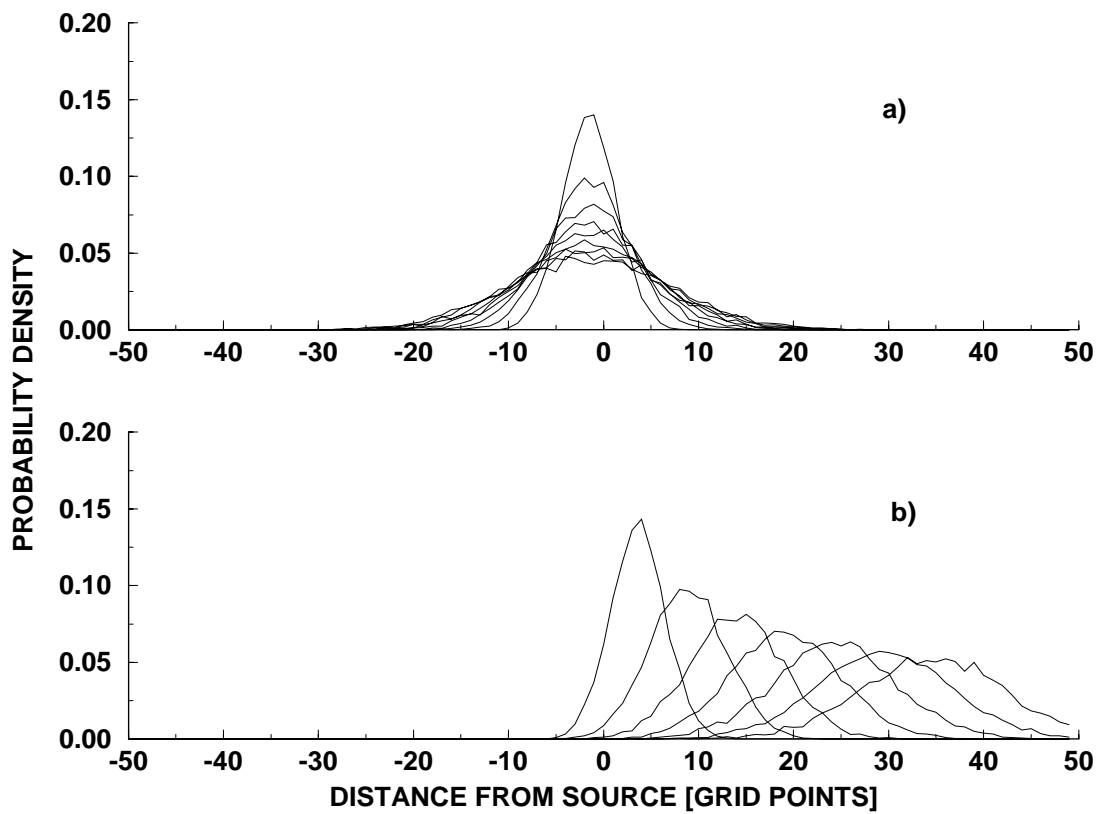


Figure 6: Probability density to find a particle at time t , location x . The initial condition is $P_{t=0, x=0} = 1$. $\Delta x = 550\text{km}$, $\Delta t = 1\text{month}$. a) diffusion only, b) diffusion plus advection (10 cm/s) 10.000 particles were used in both cases.

Figure 7: Development of mean position and standard deviation in time. The source is at the right end of the curve. The heavy line shows the mean position, the thin line standard deviation of the particle cloud. A settling velocity of $10^{-7} m/s$ is prescribed for all 10.000 particles.

Figure 8: Resulting concentration fields of the model runs described in the text. Zonal sections along 10° latitude for a) surface release and b) deep sea release. Concentrations are given in relative units (see upper bar).